

Table VI. IR Frequencies (ν , cm^{-1}), IR Intensities (I , km mol^{-1}), Raman Activities (A , $\text{\AA}^4 \text{amu}^{-1}$), and Raman Depolarization (d) Ratios for the Symmetric Stretching Mode $\nu(\text{S-H})$ for H_2S

		$\nu(\text{S-H})$	I	A	d
SCF	3-21G*	2642	2	159	0.21
SCF	6-31G**	2635	4	178	0.21
MP2	6-31G**	2591	4		

polarizability derivatives are available from the authors upon request.⁵⁵ The modes presented in Table V can be used in the analytical identification of various tautomeric forms by IR/Raman spectroscopy. The overall agreement with the matrix isolation data is reasonable. Following the data presented in Table V, the S-H mode intensity in the IR spectra should be almost two orders of magnitude smaller than that of the Raman intensity, which may suggest that the S-H mode can hardly be visible in IR but should be active in Raman. In order to understand the S-H vibrations and their activities, we performed benchmark SCF/3-21G*, SCF/6-31G**, and MP2/6-31G** calculations for the

symmetric stretching S-H mode in H_2S (Table VI). Upon examining the results, one sees that regardless of the method the IR intensities for the symmetric vibrational mode remain small. This seems to suggest that the low IR intensity of the S-H stretching in thiouracils is not an artifact of the SCF/3-21G* approximation. This would also mean that Raman will be more suitable than IR for an identification of mercapto tautomeric forms. On the other hand (somewhat surprising in view of the present study), in the low-temperature ($T = 10\text{--}14$ K) matrix-isolation IR spectra for the 4-neopentoxy-2-thiouracil, a strong single peak in the $2700\text{--}2500 \text{ cm}^{-1}$ region has been observed and interpreted as the S-H stretching.²⁷

Acknowledgment. This study was supported by an institutional grant from the National Cancer Institute and by a Biomedical Research Support grant provided by The University of Arizona. One of us, (A.L.), has been partly supported by the Polish Academy of Sciences within the project CPBP 01.12. We are indebted to Dr. K. Szczepaniak for reading the manuscript and notifying us of her latest experimental IR matrix isolation studies on thiouracils.

(55) Bitnet code LUDWIK@ARIZRVAX or ALES@ARIZRVAX.

Registry No. 2-Thiouracil, 141-90-2; 4-thiouracil, 591-28-6.

Butadiene. 1. A Normal Coordinate Analysis and Infrared Intensities. Structure of the Second Rotamer

Kenneth B. Wiberg* and Robert E. Rosenberg

Contribution from the Department of Chemistry, Yale University, New Haven, Connecticut 06511. Received July 24, 1989

Abstract: The question of the structure of the second stable conformer of butadiene (cis or gauche) has been reexamined by using a combination of theoretical and experimental methods. High level MP3/6-311+G**//MP2/6-31G* ab initio calculations predicted the gauche conformer to be energetically preferred by 0.98 kcal/mol (0.85 kcal/mol after correction for zero-point energies) over the cis conformer. Experimental data were reexamined as follows. An ab initio derived force field for *s-trans*-butadiene was fit to the observed gas-phase infrared and Raman spectra. Infrared intensities for *s-trans*-butadiene were measured and converted to dipole moment derivatives with respect to the internal coordinates, and the derivatives were compared to those obtained theoretically. The intensity data proved useful in determining the form of the normal coordinates for the out-of-plane bending modes. These data should prove useful in comparisons with force fields and dipole moment derivatives for other alkenes. The scaling factors obtained in the normal coordinate analysis were transferred to the calculated force fields for the cis and gauche forms, and the vibrational spectra were derived from these data. The ratios of dipole moment derivatives between experiment and theory, along with the calculated derivatives for the other rotamers, were used to predict intensities for both *cis*- and *gauche*-butadiene. The constructed spectra for the minor rotamers were compared to the experimental spectra. *gauche*-Butadiene was found to fit the data better than the cis conformer, in agreement with ab initio calculations. Vertical transition energies for the $\pi \rightarrow \pi^*$ ($A_g \rightarrow B_u$) transition for cis, gauche, and trans rotamers were calculated. While absolute transition energies were 5–10% too large, relative energies (with an origin corrected to *trans*-butadiene) supported a gauche conformer -5 to $+10$ nm to the red of the trans form and a cis form nearly 30 nm to the red. Although the second conformer was previously reported to be 14 nm to the red of the trans form, new experimental data suggested this gap may be only 3 nm. Significantly, both assignments of λ_{max} were in agreement with a twist angle near $25\text{--}35^\circ$. This correlation of λ_{max} to twist angle was supported empirically with the known data for cycloheptadiene and cyclooctadiene.

1. Introduction

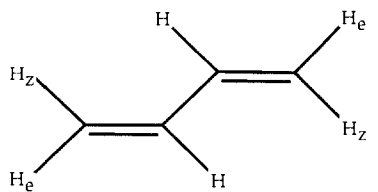
As one of the simplest of the π -conjugated systems, butadiene has received extensive study both experimentally and theoretically. Despite these studies, some important questions remain unresolved: (1) What is the structure of the second rotamer? (2) What is the origin of the 3.5 kcal/mol stabilization of butadiene which is found in hydrogenation studies?¹ (3) What is the origin of the 4–5 kcal/mol rotational barrier?² We shall attempt to answer

the first question herein, and we shall consider the other two related questions subsequently.

It has long been recognized that butadiene exists primarily in the *s-trans* form, and it has been believed that a second rotamer also exists. The question of the structure of the less stable isomer of butadiene is still in doubt. Is it *s-cis* or *s-gauche*? The structural question has been the subject of numerous experimental^{3–6} and

(1) Kistiakowsky, G. B.; Ruhoff, J. R.; Smith, H. A.; Vaughan, W. E. *J. Am. Chem. Soc.* **1935**, *57*, 876; **1936**, *58*, 146, 237.

(2) (a) Durig, T. R.; Bucy, W. E.; Cole, A. R. *Can. J. Phys.* **1976**, *53*, 1832. (b) Carriera, L. A. *J. Chem. Phys.* **1975**, *62*, 3851. (c) Lipnick, R. L.; Gorbisch, E. W. *J. Am. Chem. Soc.* **1973**, *95*, 6370.

Table I. HF/6-31G* Optimized Geometries at Fixed Torsional Angles^a


parameter	torsional angle										
	0.0	6.1	18.0	35.0	38.25	45.0	60.0	90.0	120.0	150.0	180.0
rC=C	1.3223	1.3223	1.3221	1.3215	1.3214	1.3210	1.3200	1.3186	1.3195	1.3215	1.3226
rC-C	1.4798	1.4797	1.4790	1.4783	1.4782	1.4787	1.4815	1.4893	1.4877	1.4750	1.4676
rCHz	1.0755	1.0755	1.0756	1.0757	1.0758	1.0758	1.0758	1.0762	1.0767	1.0768	1.0766
rCHe	1.0749	1.0749	1.0749	1.0752	1.0752	1.0754	1.0756	1.0757	1.0754	1.0750	1.0748
rCH	1.0776	1.0777	1.0779	1.0785	1.0786	1.0789	1.0794	1.0794	1.0784	1.0780	1.0781
∠CCC	127.16	127.10	126.68	125.69	125.52	125.16	124.69	124.49	124.28	124.13	124.12
∠HzCC	122.76	122.73	122.49	122.00	121.94	121.81	121.68	121.81	121.90	121.82	121.76
∠HeC	120.94	120.96	121.08	121.30	121.32	121.39	121.44	121.43	121.49	121.58	121.66
∠HCC	118.07	118.10	118.31	118.83	118.90	119.04	119.27	119.18	119.23	119.42	119.59
rel energy ^b	3.89	3.85	3.59	3.18	3.16	3.22	3.87	5.85	5.33	2.02	0.0

^a Distances are given in Å, angles in deg, and relative energies in kcal/mol. ^b At 180.0° $E = -154.916$ 54H.

theoretical studies.⁷⁻⁹ Experimental resolution of this question is not straightforward as the energy difference between the two forms is 2.5–3.1 kcal/mol, which means that at room temperature only about 1% of the less stable conformer will be present. This problem was first circumvented by Huber-Wälchli and Günthard¹⁰ who heated butadiene up to 800 K, giving a significant Boltzmann population of the less stable form (~15%). The mixture was then quickly cooled below 20 K which trapped the high-temperature distribution, without allowing the mixture to reequilibrate (the activation barrier for this is about 4 kcal/mol). This method allowed Squillacote, Sheridan, Chapman, and Anet (SSCA)^{4a} to record the infrared and ultraviolet spectrum of the minor conformer. The λ_{\max} of the second conformer was found to be 14 nm to the red of the trans. Pariser-Parr calculations suggested a blue shift for the gauche rotamer, and therefore the minor rotamer was assigned the cis conformation. Later, Furakawa et al.³ carried out a detailed normal coordinate analysis with the d_0 , d_4 , and d_6 butadiene minor conformers which suggested the gauche form. Subsequently, Squillacote, Semple, and Mui^{4b} argued for a cis form on the basis of more UV data concerning dimethylbutadienes, and their conclusions were supported by Fisher and Michl's elegant polarization study.⁵

Many theoretical studies have been carried out. Two recent studies led to different conclusions. One found the gauche form to be 0.7 kcal/mol more stable than cis,⁷ and the other concluded that theory could not distinguish unambiguously between the two forms.⁸ We felt that by extending the theory and reexamining the experimental data, we might arrive at a consistent prediction for the torsional angle between the two double bonds in the minor form of butadiene.

We have calculated the structures and energies of butadiene rotamers including electron correlation. We have reexamined the vibrational force field of the trans form making use of new experimental data combined with a theoretically determined force field. Dipole moment derivatives have been obtained from measured infrared intensities. They have been used to calculate atomic polar tensors, which are helpful in comparing intensity data between similar molecules. The infrared spectra of gauche- and

cis-butadienes were calculated theoretically and scaled to form an experimental spectrum by using the scaling factors derived from the fitting of trans-butadiene with use of both line transitions and intensities. The simulated spectra have been compared with the available experimental data. Electronic absorption vertical transitions for the various conformers of butadiene were calculated and compared to experiment. The predicted spectra are discussed within the context of the known λ_{\max} of cycloheptadiene and cyclooctadiene.

2. Theoretical Studies

The most recent ab initio studies have reached different conclusions. The first, reported by Breulet, Lee, and Schaefer⁷ used a double- ζ plus polarization (DZ+P) fully optimized geometry and included configuration interaction using all single and double excitations at the DZ+P geometry (SD-CI). They found that gauche-butadiene was energetically preferable to the cis form by 0.7 kcal/mol. Davidson and Feller,⁸ 2 years later, reported optimized MCSCF energies with use of the Dunning-Hay SV basis set and found that the cis form was 120 cal/mol more stable than the gauche. However, this conclusion is tempered by the fact that the inclusion of polarization functions in going from DZ + DZ+P at the DZ optimized geometries resulted in a 420 cal/mol bias favoring the gauche compound. The authors noted that inclusion of polarization functions to give MCSCF DZ+P optimized structures may favor the gauche form. They said that any predictions made by using such small energy differences "should be viewed with a certain amount of skepticism". Thus current theory leans toward the gauche form but not unambiguously.

We sought to clarify the problem by trying to include in our computational methods tools that would accurately reproduce factors of import to this question. Presumably, the energetic preference for gauche- versus cis-butadiene is due to the severe steric interactions between the inner hydrogens on C1 and C4 as can be seen from a comparison of the bond angles in the cis and trans forms (Table I). Bond lengths at the 6-31G* level of theory are known to be about 1% too short.¹¹ This bond compression would heighten the steric problems in the cis form. Correction for electron correlation using the Møller-Plesset perturbation theory through the second-order (MP2)¹² is known to reproduce

(3) Furakawa, Y.; Takenchi, H.; Harada, I.; Tasumi, M. *Bull. Chem. Soc. Jpn.* **1983**, *56*, 392.

(4) (a) Squillacote, M. E.; Sheridan, R. S.; Chapman, O. L.; Anet, F. A. L. *J. Am. Chem. Soc.* **1979**, *101*, 3657. (b) Squillacote, M. E.; Semple, T. C.; Mui, P. W. *J. Am. Chem. Soc.* **1985**, *107*, 6842.

(5) Fisher, J. J.; Michl, J. *J. Am. Chem. Soc.* **1987**, *109*, 1056.

(6) Mui, P. W.; Grunwald, E. *J. Am. Chem. Soc.* **1982**, *104*, 6562.

(7) Breulet, J.; Lee, T. J.; Schaefer III, H. F. *J. Am. Chem. Soc.* **1984**, *106*, 6250.

(8) Feller, D.; Davidson, E. R. *Theor. Chem. Acta* **1985**, *68*, 57.

(9) (a) Bock, C. W.; George, P.; Trachtman, M. *Theor. Chim. Acta* **1984**, *64*, 293. (b) Kavana-Saebø, K.; Saebø, S.; Boggs, J. E. *J. Mol. Struct.* **1984**, *106*, 259. (c) Tai, J. C.; Allinger, N. L. *J. Am. Chem. Soc.* **1976**, *98*, 7928. (d) Radom, L.; Pople, J. A. *J. Am. Chem. Soc.* **1970**, *92*, 4786.

(10) Huber-Wälchli, P. *Ber. Bunsenges Phys. Chem.* **1978**, *82*, 10. Huber-Wälchli, P.; Günthard, H. H. *Spectrochim. Acta* **1981**, *37A*, 285.

(11) (a) DeFrees, D. J.; Ragavachari, K.; Schlegel, H. B.; Pople, J. A. *J. Am. Chem. Soc.* **1982**, *104*, 5576. (b) Wiberg, K. B. *J. Org. Chem.* **1985**, *50*, 5285.

Table II. MP2/6-31G* Optimized Geometries at Fixed Torsional Angles

parameter	torsional angle										obs ¹⁴
	0.0	18.0	35.0	37.87	45.0	60.0	90.0	120.0	150.0	180.0	
rC=C	1.3426	1.3422	1.3414	1.3411	1.3408	1.3395	1.3381	1.3389	1.3412	1.3425	1.341
rC-C	1.4670	1.4690	1.4686	1.4696	1.4690	1.4730	1.4813	1.4789	1.4645	1.4562	1.463
rCHz	1.0856	1.0857	1.0857	1.0857	1.0856	1.0855	1.0855	1.0860	1.0863	1.0863	1.090
rCHe	1.0842	1.0842	1.0845	1.0845	1.0847	1.0850	1.0850	1.0848	1.0844	1.0844	1.090
rCH	1.0884	1.0887	1.0892	1.0892	1.0896	1.0899	1.0902	1.0894	1.0894	1.0897	1.090
∠CCC	126.47	125.86	124.60	124.36	123.95	123.46	123.56	123.51	123.61	123.71	123.3
∠HzCC	122.46	122.14	121.54	121.39	121.30	121.14	121.47	121.55	121.46	121.44	121.8
∠HeCC	121.04	121.20	121.49	121.58	121.58	121.63	121.51	121.57	121.72	121.77	121.8
∠HCC	117.91	118.22	118.83	118.98	119.14	119.36	119.21	119.24	119.43	119.56	121.8
rel energy ^a	3.59	3.27	2.85	2.84	2.92	3.68	5.78	5.25	1.98	0.0	

^a At 0.0° $E = -155.43599H$ (MP2/6-31G*); $-155.55603H$ (MP3/6-311+G**); at 37.87° $E = -155.43719H$ (MP2/6-31G*), $-155.55760H$ (MP3/6-311+G**).

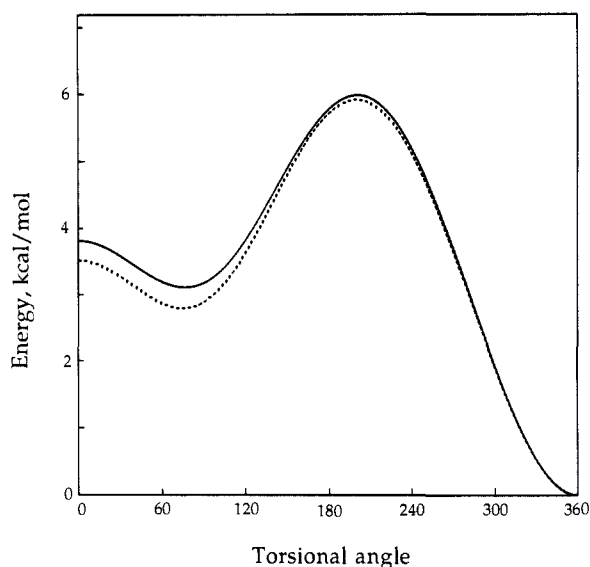


Figure 1. Energies of butadiene rotamers as a function of the C-C-C torsional angle. The solid line gives the HF/6-31G* energy changes, and the dashed line gives the MP2/6-31G* energies.

experimental bond lengths quite well,¹³ possibly alleviating some of the steric problems. After this work was completed, Bock and Panchenko¹⁴ reported the MP2/6-31G* structures and energies for *cis*- and *gauche*-butadiene, leading to results and conclusions which are in complete agreement with the following.

The MP2/6-31G* calculated structure for *trans*-butadiene is compared with the experimental structure¹⁵ in Table II, and a good agreement is found. As can be seen from Tables I and II and Figure 1; the MP2/6-31G* torsional potential appears nearly identical with the 6-31G* potential and was in favor of the *gauche* form ($\Delta E = 0.75$ kcal/mol). More extensive correction for electron correlation and the use of larger basis sets would probably have only a small effect on geometries (most of this having been taken into account in the MP2 optimizations) but may favor one form or the other energetically. Thus the basis set was expanded to triple- ζ quality with diffuse functions on carbon and polarization functions on all atoms -6-311+G**. The stabilizing interaction of coplanar double bonds in *s-cis*-butadiene, to be discussed more fully in a subsequent publication, would almost surely benefit from this larger basis set, while a smaller effect was expected for the *s-gauche* structure. Nonetheless, the MP3/6-311+G**//MP2/6-31G* energies favored the *gauche* form over *cis* by 0.98 kcal/mol. Correction for the differences in zero-point energies with use of the data presented below gave a barrier of 0.85

kcal/mol. Interestingly, as electron correlation was added, and then the basis set enlarged, the torsional potential remained surprisingly the same. We thus conclude that theory predicts *gauche* to be the second stable form of butadiene and furthermore that higher levels of theory will not reverse this ordering. Due to numerous past successes with theory in this type of problem,¹⁶ it seems unlikely that theory would be wrong in this case. Can the experimental data be interpreted as consistent with the theory?

3. Vibrational Spectra

The spectra of the second stable form of butadiene have been examined by several groups, who came to different conclusions. Furakawa et al. favored a *gauche* form based on the infrared spectrum but suggested that the *cis* form is an adequate model,³ while SSCA used ultraviolet absorption studies to support a *cisoid* structure.^{4a}

The vibrational spectrum of *s-trans*-butadiene has been studied many times, and several normal coordinate analyses have been reported.¹⁷ However, the interpretation of the spectrum has been difficult because of the well-known problem of determining a unique force field for polyatomic molecules of more than four or five atoms. Only $3N - 6$ pieces of data come from each isotopomer, while $(N)(N + 1)/2$ pieces of data are needed to uniquely define the force field. Furthermore, reducing the potential energy F matrix by employing symmetry and obtaining additional data through the use of isotopomers, methods used for small molecules, does not yield enough data for a unique force field determination. While it may appear that generating enough isotopomers would eventually clarify the force field, product rules relating isotopomers reduce the number of unique data available from each species. We have therefore employed theoretical calculations as a starting point for a normal coordinate analysis.

There is a clear consensus as to the vibrational assignment for butadiene.¹⁷ However, the previous work was unsatisfactory for our purposes because most of the Raman data were obtained in the liquid phase, and it is known that there are shifts in band positions on going from the liquid to the gas phase. In order to have a consistent set of data, all obtained in the gas phase, we have redetermined the band positions. Butadiene- d_0 , -2,3- d_2 , -1,1,4,4- d_4 , and - d_6 isomers were thus reexamined. Their synthesis followed literature procedures,¹⁸ and purity was determined by

(16) Wiberg, K. B.; Murcko, M. A. *J. Am. Chem. Soc.* **1988**, *110*, 8029. Wiberg, K. B.; Murcko, M. A. *J. Mol. Struct.* **1988**, *163*, 1. Wiberg, K. B.; Murcko, M. A. *J. Phys. Chem.* **1987**, *91*, 3616. Wiberg, K. B.; Laidig, K. E. *J. Am. Chem. Soc.* **1987**, *109*, 5935.

(17) (a) Sverdlov, L. M.; Tarasova, N. V. *Optics and Spectroscopy*; **1960**, *9*, 159. (b) Marais, D. J.; Sheppard, N.; Stoicheff, B. P. *Tetrahedron* **1962**, *17*, 163. (c) Cole, A. R. H.; Mohay, G. M.; Osborne, G. A. *Spectrochem. Acta* **1967**, *32A*, 909. (d) Panchenko, Y. N.; Pulay, P.; Torok, F. *J. Mol. Struct.* **1976**, *34*, 283. (e) Panchenko, Y. N. *Spectrochem. Acta* **1975**, *31A*, 1201. (f) Bondybyev, V. E.; Nibler, J. W. *Spectrochem. Acta* **1973**, *29A*, 645. (g) Cole, A. R. H.; Green, A. A.; Osborne, G. A. *J. Mol. Spectrosc.* **1973**, *48*, 212. (h) Benedetti, E.; Aglietto, M.; Pucci, S.; Panchenko, Y.; Pentin, Y. A.; Nikitin, O. T. *J. Mol. Struct.* **1978**, *49*, 293. (i) Bock, C. W.; Trachtman, M. *J. Mol. Spectrosc.* **1980**, *84*, 243. (j) Caralp, L.; Dussubieux, M. *J. Mol. Struct.* **1976**, *35*, 289. (k) Abe, K. Ph.D. Thesis, Tokyo University, Tokyo, Japan, 1970.

(18) Charlton, J. L.; Agagnier, R. *Can. J. Chem.* **1973**, *51*, 1852.

(12) Møller, C.; Plesset, M. S. *Phys. Rev.* **1934**, *46*, 618. Binkley, J. S.; Pople, J. A. *Int. J. Quantum Chem.* **1975**, *9*, 229. Pople, J. A.; Binkley, J. S.; Seger, R. *Int. J. Quantum Chem. Symp.* **1976**, *10*, 1.

(13) Hehre, W.; Radom, L.; Schleyer, P. v. R.; Pople, J. A. *Ab Initio Molecular Orbital Theory*; Wiley: New York, 1986; p 155ff.

(14) Bock, C. W.; Panchenko, Y. N. *J. Mol. Struct.* **1989**, *187*, 69.

(15) Kuchitsu, K.; Fukuyama, T.; Morino, Y. *J. Mol. Struct.* **1967**, *1*, 463.

Table III. Calculated and Observed Vibrational Spectra (cm⁻¹) for Butadiene

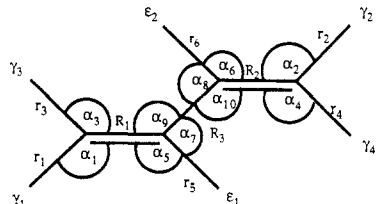
species	calc	<i>d</i> ₀		2,3- <i>d</i> ₂			1,1,4,4- <i>d</i> ₄			<i>d</i> ₆					
		scaled	obs	calc	scaled	obs	calc	scaled	obs	calc	scaled	obs			
Ag	ν_1	3415	3108	3100	3414	3107	3099	3336	3036	3013	2545	2316	2343		
	ν_2	3343	3042	3013	3334	3034	3005	2545	2315	2316	2487	2263	2266		
	ν_3	3326	3027	3013	2472	2250	2249	2444	2224	2225	2428	2210	2212		
	ν_4	1898	1670	1644	1870	1645	1613	1851	1629	1613	1818	1600	1589		
	ν_5	1614	1420	1441	1596	1401	1428	1446	1273	1296	1303	1146	1192		
	ν_6	1435	1263	1277	1344	1182	1220	1278	1125	1167	1160	1021	1046		
	ν_7	1326	1167	1203	1038	913	934	1158	1019	1040	1019	897	918		
	ν_8	960	844	888	951	837	880	800	704	740	799	703	738		
	ν_9	550	484	512	535	470	496	489	430	452	479	419	439		
Au	ν_{10}	1161	1022	1014	1069	941	908	1089	958	955	884	778	766 ^b		
	ν_{11}	1069	941	908	973	857	850	854	751	728	831	731	719		
	ν_{12}	582	512	525	534	470	480	440	387	404 ^b	426	375	391 ^b		
	ν_{13}	167	147	162 ^a	156	138		153	135	149 ^a	144	127	142 ^a		
Bg	ν_{14}	1117	983	965	1073	857	913	1075	946	930	924	813	793		
	ν_{15}	1068	940	908	930	819	820	853	751	728	812	714	700		
	ν_{16}	852	750	752	844	743	745	688	605	610 ^a	677	596	603 ^a		
Bu	ν_{17}	3415	3108	3101	3414	3107	3098	3344	3043	3020	2545	2316	2350		
	ν_{18}	3343	3043	3055	3334	3034	3031	2544	2315	2332	2484	2260	2266		
	ν_{19}	3332	3033	2984	2470	2248	2243	2446	2226	2226	2430	2211	2220		
	ν_{20}	1819	1600	1597	1804	1588	1586	1736	1528	1533	1718	1512	1520		
	ν_{21}	1547	1361.2	1381	1540	1355	1374	1411	1242	1275	1162	1022	1048		
	ν_{22}	1438	1265.8	1294	1248	1098	1127	1143	1006	1030	1113	980	1005		
	ν_{23}	1089	958	990	927	815		895	787	813	815	717	730		
	ν_{24}	319	281	301 ^b	307	270		276	243	258 ^b	268	236	250 ^b		
rms error = 27				rms error = 25				rms error = 20				rms error = 20			

^aReference 16g. ^bReference 16k.

both NMR and IR. The infrared spectra were obtained with a Nicolet 7199 spectrometer at 0.25-cm⁻¹ resolution by using a 7.25 cm gas cell. The Raman spectra were measured in the gas phase with 2-cm⁻¹ resolution by using a Spex 1403 Ramalog.

As would be expected most vibrational frequencies were in accord with literature values. Only one significant change was made: ν_{18} of the light compound was assigned to 2984 cm⁻¹ by Panchenko^{17d,e} and 3031 cm⁻¹ by us. Both bands appeared in the *d*₁ and *d*₂ species. The higher energy band was assigned to ν_{18} because it fits both the force field for butadiene and was consistent with the intensity data, vide infra. We note that ν_{17} of the *d*₄ compound was at 3020 cm⁻¹, which is the exact midpoint of ν_{18} and ν_{19} in the parent. One possibility is that these two bands interact in a first order sense in the parent and that when this interaction is removed by deuteration in the *d*₂ case the band shifts to higher energy. We assigned the 2984-cm⁻¹ band to the 8% residual *d*₁ in the *d*₂ compound (present in both laboratories, since the method of preparation was the same). Additionally, ν_{17} of the *d*₄ compound was reported at 3037 and 3041 cm⁻¹, while we found it at 3020 cm⁻¹. As this band was quite strong and the only band present, we attribute this to a poor choice of band origin in the lower resolution spectra. It should be noted that these two discrepancies do not significantly change the fit force field, due to the identical assignments on the more than 80 other bands.

A harmonic force field was calculated by using ab initio methods at the 6-31G* level of theory.¹⁹ Due to bond shortness, leading to higher force constants, the problem of anharmonicity, and the limitations of ab initio methods (basis set incompleteness, lack of electron correlation), the frequencies calculated are generally found to be about 10% higher than the observed anharmonic frequencies. The calculated spectra for the four isotopomers are compared with the experimental data in Table III. We have found that a simple scaling scheme (0.91 for CH stretches, 0.88 for all other frequencies) normally results in an RMS error of less than 25 cm⁻¹.²⁰ This was also found to be the case with butadiene.

Table IV. Symmetry Coordinates for Butadiene^a


Ag	$S_1 = R_1 + R_2$	Bg	$S_{14} = \gamma_1 - \gamma_2 + \gamma_3 - \gamma_4$
	$S_2 = R_3$		$S_{15} = \gamma_1 - \gamma_2 - \gamma_3 + \gamma_4$
	$S_3 = r_1 + r_2$	Bu	$S_{16} = \epsilon_1 - \epsilon_2$
	$S_4 = R_3 + r_4$		$S_{17} = R_1 - R_2$
	$S_5 = r_5 + r_6$		$S_{18} = r_1 - r_2$
	$S_6 = \alpha_1 + \alpha_2$		$S_{19} = r_3 - r_4$
S	$S_7 = \alpha_3 + \alpha_4$		$S_{20} = r_5 - r_6$
	$S_8 = \alpha_5 + \alpha_6 - \alpha_7 - \alpha_8$		$S_{21} = \alpha_1 - \alpha_2$
	$S_9 = \alpha_9 + \alpha_{10}$		$S_{22} = \alpha_3 - \alpha_4$
Au	$S_{10} = \gamma_1 + \gamma_2 - \gamma_3 - \gamma_4$		$S_{23} = \alpha_5 - \alpha_6 - \alpha_7 + \alpha_8$
	$S_{11} = \gamma_5$		$S_{24} = \alpha_9 - \alpha_{10}$
	$S_{12} = \gamma_1 + \gamma_2 + \gamma_3 + \gamma_4$		
	$S_{13} = \epsilon_1 + \epsilon_2$		

^aThe γ 's are HCCC torsional angles, and the ϵ 's are CH out-of-plane bending coordinates.

The calculated force constants were then adjusted to give a "best fit" to the observed spectrum based on the symmetry coordinates given in Table IV and the experimental geometry. The fitting procedure used one scaling factor for each diagonal **F** matrix element and one for all the off-diagonal elements in a given symmetry block for 28 in all. This reduced the rms error to only 10 cm⁻¹ with much of the error coming from the highly anharmonic CH stretches (Table V). In fact, without the CH stretches the rms error of the fit was less than 3 cm⁻¹. The scaling factors and force constants are summarized in Table VI. It should be noted that scaling factors (ratio of fit to calculated) were almost uniformly near 0.8 (mean = 0.8304, *s* = 0.080). The narrowness of their spread is necessary though not sufficient to show that the calculation is qualitatively correct and that the data is not fit from just a random force field.

The force constants reported by Furakawa et al.³ are also given in Table VI. There are significant differences between their values and those obtained in this investigation. This resulted in large measure from the necessity in the previous work of setting many

(19) (a) Pulay, P.; Fogarasi, G.; Pongor, G.; Boggs, J.; Vargha, A. *J. Am. Chem. Soc.* **1983**, *105*, 7037. (b) Hess, B. J., Jr.; Schaad, L. J.; Carsky, P.; Zahradnik, R. *Chem. Rev.* **1986**, *86*, 709.(20) (a) Wiberg, K. B.; Dempsey, R. C.; Wendolowski, J. J. *J. Phys. Chem.* **1984**, *88*, 5596. (b) Wiberg, K. B. *J. Am. Chem. Soc.* **1979**, *101*, 1718. (c) Wiberg, K. B.; Walters, V. A.; Dailey, W. P. *J. Am. Chem. Soc.* **1985**, *107*, 4860. (d) Wiberg, K. B.; Walters, V. A.; Wong, K. N.; Colson, S. D. *J. Phys. Chem.* **1984**, *88*, 6067. (e) Wiberg, K. B.; Walters, V.; Colson, S. D. *J. Phys. Chem.* **1984**, *88*, 4723.

Table V. Fit and Observed IR Spectra for Butadiene

species		d_0			$2,3-d_2$			$1,1,4,4-d_4$			d_6		
		calc	fit	obs	calc	fit	obs	calc	fit	obs	calc	fit	obs
Ag	ν_1	3415	3109.4	3100.3	3414	3108.8	3098.8	3336	3022.4	3012.8	2545	2318.4	2343.3
	ν_2	3343	3027.5	3013.0	3334	3020.6	3005.3	2545	2318.3	2315.8	2487	2249.6	2265.6
	ν_3	3326	3014.5	3013.0	2472	2240.8	2249.3	2444	2205.9	2224.6	2428	2195.9	2211.8
	ν_4	1898	1650.1	1643.9	1870	1619.0	1613.3	1851	1617.2	1613.3	1818	1577.8	1588.6
	ν_5	1614	1449.2	1440.8	1596	1426.6	1428.2	1446	1295.3	1296.4	1303	1195.6	1192.3
	ν_6	1435	1282.4	1276.5	1344	1230.0	1220.1	1278	1170.7	1167.4	1160	1040.5	1045.7
	ν_7	1326	1206.3	1203.0	1038	928.1	934.4	1158	1032.6	1039.8	1019	909.0	917.5
	ν_8	960	884.6	887.8	951	876.3	880.4	800	733.0	738.8	799	731.6	738.0
	ν_9	550	506.1	511.6	535	492.7	495.5	489	451.0	452.0	479	439.9	438.5
Au	ν_{10}	1161	1015.8	1014.0	1069	913.2	908.4	1089	952.2	955.2	884	773.5	766 ^a
	ν_{11}	1069	910.0	908.1	973	852.1	850.0	854	726.4	728.1	831	708.1	718.6
	ν_{11}	1069	910.0	908.1	973	852.1	850.0	854	726.4	728.1	831	708.1	718.6
	ν_{12}	582	524.1	524.6	534	480.2	480.7	440	396.7	404 ^a	426	384.6	391 ^a
	ν_{13}	167	162.0	162.5	156	138	138	153	148.3	149.2	144	127	142 ^b
Bg	ν_{14}	1117	968.7	965.4	1073	916.8	912.6	1075	928.7	930.0	924	813	793.4
	ν_{15}	1068	909.4	908.0	930	808.9	810.0	853	725.3	728.2	812	691.9	700.0
Bu	ν_{16}	852	754.9	751.9	844	741.6	745.1	688	612.4	610 ^a	677	602.9	603 ^a
	ν_{17}	3415	3118.4	3100.6	3414	3117.6	3098.4	3344	3014.9	3019.7	2545	2325.6	2349.5
	ν_{18}	3343	3042.1	3054.8	3334	3041.3	3031.1	2544	2325.1	2332.2	2484	2247.6	2266.0
	ν_{19}	3332	3012.9	2984.1	2470	2228.8	2242.5	2446	2223.7	2225.5	2430	2203.3	2219.8
	ν_{20}	1819	1606.2	1596.5	1804	1592.9	1586.1	1736	1530.9	1532.6	1718	1512.8	1519.5
	ν_{21}	1547	1380.4	1380.7	1540	1380.4	1380.7	1411	1271.4	1275.3	1162	1049.8	1047.8
	ν_{22}	1438	1294.2	1294.2	1248	1132.9	1127.0	1143	1023.8	1029.8	1113	1002.8	1005.3
	ν_{23}	1086	982.1	990.3	927	832.5	895	895	813.5	812.7	815	735.0	729.9
	ν_{24}	319	335.9	301 ^a	307	323.0	276	276	288.4	258 ^a	268	279.8	250 ^a

rms error = 9.5

rms error = 8.2

rms error = 5.8

rms error = 12.2

^a Reference 17k. ^b Reference 17g.

of the off-diagonal terms to zero. The present results show that in many cases this assumption was not satisfactory.

4. Intensity Data

Information on the infrared band intensities was desired for two reasons. First, they are of value in testing vibrational force fields and give information on charge distributions in molecules.²¹ Second, in the present case, they would be useful in predicting the band intensities of the *cis* and *gauche* forms of butadiene. Empirically, *ab initio* intensities frequently have errors of ± 20 –50% as compared to the actual intensities and are only a rough guide as to actual observed intensities.²² We hoped to reduce some of this uncertainty by scaling the calculated intensities for the *trans* compound to the actual observed intensities and by using these scaling factors to better predict intensities for the *cis* and *gauche* form from the calculated data. While we hope to predict intensities as accurately as possible, it is also important to see how well intensity data from one molecule (*trans*-butadiene) transfers to similar molecules (*cis*- and *gauche*-butadiene). In the past, force field data has been transferred from one molecule to another successfully,²³ and we hoped intensity data would behave similarly.

Unfortunately, infrared intensity data are quite scarce, due in no small part to the experimental difficulties. We have measured for the first time the absolute infrared intensities of the four isotopic butadienes in the gas phase at 0.25-cm⁻¹ resolution following the Wilson–Wells–Penner procedure.²⁴ A brass high-pressure cell similar to that described by Dickson et al.²⁵ with a path length of 72.5 mm was used for all measurements. The spectra were obtained at a pressure of 300 psi of nitrogen in order to broaden the rotational lines and were obtained for a range of butadiene partial pressures. Care was taken such that at least five pressures were available for all bands (strong bands saturate the signal and must be measured at lower pressures, while weak

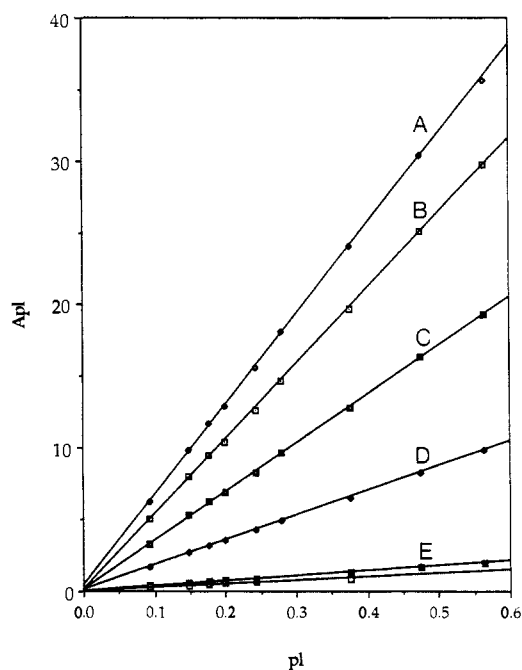


Figure 2. Beer's law plots of Apl (km-atm/mol-cm) against pl (atm-cm) for butadiene- d_0 . The integration regions were as follows: A, 800–967 cm⁻¹; B, 2850–3225 cm⁻¹; C, 967–1125 cm⁻¹; D, 1525–1650 cm⁻¹; E, 1337–1408 cm⁻¹; and F, 1200–1337 cm⁻¹.

bands need higher pressures for adequate signal to noise). In each case, Beer's law plots were linear (Figure 2). The intensity data are given in Table VII.

As is frequently observed, some of the infrared bands overlap, and it was necessary to find a way in which to obtain the individual band contributions. Three methods were employed to solve this problem. A cut and weigh method, which is clearly a subjective determination, was used to deconvolute intensity in all cases. In some cases, the ratio of the bands could be obtained from solution-phase spectra where the bands were relatively narrow because the rotational structure has been eliminated. This was effective for only those bands without severe overlap problems and gave results which agreed well with the cut and weigh method above.

(21) Wiberg, K. B.; Wendoloski, J. J. *J. Phys. Chem.* **1984**, *88*, 586.(22) Miller, M. D.; Jensen, F.; Chapman, O. L.; Houk, K. N. *J. Phys. Chem.* **1989**, *93*, 4495.(23) Sellers, H.; Pulay, P.; Boggs, J. E. *J. Am. Chem. Soc.* **1985**, *107*, 6487.(24) (a) Wilson, E. B., Jr.; Wells, A. J. *J. Chem. Phys.* **1946**, *14*, 578. (b) Penner, S. S.; Weber, D. *J. Chem. Phys.* **1951**, *19*, 807. (c) Overend, J.; Younquist, M. J.; Curtis, E. C.; Crawford, B., Jr. *J. Chem. Phys.* **1959**, *30*, 532.(25) Dickson, A. D.; Mills, I. M.; Crawford, B. *J. Chem. Phys.* **1957**, *27*, 445.

Table VI. Force Constants for Butadiene Using Symmetry Coordinates

A. Diagonal Force Constants, mdynes/Å					
	calc force constants	scaling factors	adjusted force constants	previous force constants ³	
A _g	1,1	11.17	0.716	8.01	8.79
	2,2	5.85	0.843	4.93	5.43
	3,3	6.21	0.819	5.09	5.06
	4,4	6.29	0.831	5.22	5.06
	5,5	6.12	0.820	5.02	5.00
	6,6	1.15	0.827	0.95	0.52
	7,7	1.15	0.839	0.97	0.52
	8,8	0.69	0.831	0.57	0.56
	9,9	1.44	0.871	1.25	0.76
A _u	10,10	0.42	0.754	0.32	0.30
	11,11	0.12	0.934	0.11	0.11
	12,12	0.30	0.820	0.25	0.49
B _g	13,13	0.74	0.794	0.59	0.40
	14,14	0.42	0.759	0.32	0.30
B _u	15,15	0.33	0.810	0.27	0.53
	16,16	0.63	0.787	0.49	0.41
	17,17	11.35	0.772	8.77	8.99
	18,18	6.21	0.839	5.22	5.06
	19,19	6.28	0.827	5.19	5.06
	20,20	6.12	0.812	4.97	5.00
	21,21	1.15	0.825	0.95	0.52
	22,22	1.14	0.831	0.94	0.52
	23,23	0.59	0.819	0.48	0.48
24,24	1.07	1.150	1.23	0.62	

B. Off Diagonal Force Constants^a

Ag scaling factor = 0.774								
	2	3	4	5	6	7	8	9
1	0.44 (0.57)	0.08	0.08	0.10	0.21 (-0.14)	0.23 (-0.14)	0.17 (0.23)	0.22 (0.26)
2		0.00	0.00	0.08	-0.02	0.05	-0.21 (-0.32)	0.23 (0.11)
3			0.04 (0.01)	0.01	-0.01	0.12	0.02	-0.06
4				0.01	-0.12	0.01	0.00	0.06
5					0.04	0.01	-0.02	-0.17
6						0.40 (-0.06)	0.04 (0.03)	-0.03
7							-0.01 (-0.05)	0.10
8								0.04
A _u scaling factor = 0.786				B _g scaling factor = 0.791				
	11	12	13	15	16			
10	0.00	-0.01	-0.04	14	0.01	0.04		
11		0.02	-0.07	15		-0.21		
12			0.22					
B _u scaling factor = 0.819								
	18	19	20	21	22	23	24	
17	0.09	0.07	0.07	0.23 (-0.14)	0.23 (-0.14)	0.16 (0.23)	0.09 (0.26)	
18		0.04	-0.01	0.00	-0.13	0.04	-0.06	
19			0.01	-0.13	-0.02	-0.01	0.04	
20				0.03	-0.02	0.02	-0.08	
21					0.42	0.06	-0.04	
22						-0.01	0.06	
23							0.02	

^aThe previously reported (ref 3) off diagonal constants are given in parentheses. All of the others were previously assigned as zero.

As shown in Table VIII, the ratio of intensity as calculated ab initio was close to the subjective method above, and, in the absence of other data, the ratio of calculated intensities were used to separate the components of severely overlapped bands.

It should be noted that for each intensity datum, there are two choices of sign for $d\mu/dQ$ since the intensity is proportional to the square of this quantity. Moreover, if polarization is not along a unique axis, as is the case with butadiene, it is impossible to partition intensity between the unique directions. This problem

Table VII. Intensities of Infrared Bands

iso-topomer	region (cm ⁻¹)	slope (km/mol)	R	% error in slope	bands
d ₀	3225-2850	52.43	0.9999	0.31	$\nu_{17}, \nu_{18}, \nu_{19}$
	1650-1525	17.33	0.9999	0.44	ν_{20}
	1408-1337	3.49	0.9999	0.47	ν_{21}
	1337-1200	2.37	0.9950	5.06	ν_{22}
	1125-967	34.10	0.9999	0.45	ν_{10}, ν_{23}
d ₂	967-800	63.01	0.9999	0.64	ν_{11}
	3200-2875	32.64	0.9998	0.77	ν_{17}, ν_{18}
	2350-2150	8.55	0.9999	0.61	ν_{19}
	1640-1525	18.56	0.9998	0.97	ν_{20}
	1450-1332	4.58	0.9998	0.96	ν_{21}
d ₄	1300-1055	1.53	0.9885	7.17	ν_{22}
	1300-980	3.66	0.9970	3.63	ν_{22}
	1300-700	72.45	0.9995	1.52	$\nu_{10}, \nu_{11}, \nu_{22}, \nu_{23}$
	3100-2920	18.2	0.9999	0.72	ν_{17}
	2500-2274	8.71	0.9993	1.57	ν_{18}
d ₆	2500-2125	13.15	0.9994	1.50	ν_{18}, ν_{19}
	1570-1500	10.1	0.9998	0.84	ν_{20}
	1300-1240	0.7	0.9993	1.68	ν_{21}
	1300-1000	5.07	0.9998	0.95	ν_{21}, ν_{22}
	1100-840	28.87	0.9995	1.51	ν_{10}, ν_{22}
d ₆	840-625	41.17	0.9998	0.73	ν_{11}, ν_{23}
	2441-2110	23.09	0.9996	0.41	$\nu_{17}, \nu_{18}, \nu_{19}$
	1650-1482	12.94	0.9996	0.49	ν_{20}
	1228-904	7.14	0.9996	0.90	ν_{21}, ν_{22}
	810-625	51.45	0.9995	0.89	ν_{11}, ν_{23}

Table VIII. Intensity Partitioning for Butadiene

range	band origin	obs intensity	%	ab initio intensity	%
a. Butadiene-d ₀					
3225-2850	ν_{17}	28.5	54.6	44.73	49.4
	ν_{18}	12.8	24.5	15.69	17.3
	ν_{19}	10.9	20.8	30.09	33.2
1650-1525	ν_{20}	17.33		16.35	
	ν_{21}	2.96		2.34	
	ν_{22}	1.94		2.85	
1408-1337 ^a	ν_{10}	32.4	95.1	29.94	92.9
	ν_{23}	1.7	4.9	2.28	7.1
	ν_{11}	63.01		103.26	
967-800	ν_{12}	16.18		11.31	
	ν_{12}	16.18		11.31	
b. Butadiene-d ₂					
3200-2875 ^a	ν_{17}	17.9	65.1	35.00	61.2
	ν_{18}	9.6	34.9	22.19	38.8
	ν_{19}	8.55		17.48	
2350-2180	ν_{20}	18.56		16.50	
	ν_{21}	4.58		2.87	
	ν_{22}	1.53		4.29	
1640-1525	ν_{10}	68.9	95.1	99.72	86.6
	ν_{11}	3.6	4.9	15.12	13.1
	ν_{23}	na		0.26	0.2
c. Butadiene-d ₄					
3100-2936	ν_{17}	18.2		34.25	
	ν_{18}	8.7		17.23	
	ν_{19}	4.45		7.31	
2500-2271	ν_{20}	10.1		13.22	
	ν_{21}	0.7		0.79	
	ν_{22}	4.37		4.02	
1581-1385	ν_{10}	24.5		26.25	
	ν_{23}	1.4		3.50	
	ν_{11}	39.8		67.57	
d. Butadiene-d ₆					
2440-2110	ν_{17}	10.1	43.7	22.17	51.5
	ν_{18}	3.2	13.8	6.67	15.5
	ν_{19}	9.8	42.4	14.20	33.0
1650-1482 ^a	ν_{20}	11.8		13.28	
	ν_{21}	1.0	23.4	0.41	6.1
	ν_{22}	3.2	76.6	6.26	93.9
1228-904 ^a	ν_{23}	50.1	97.3	70.83	98.0
	ν_{11}	1.4	2.7	1.44	2.0

^aAn overtone or combination band contributed to the measured intensity in this region.

Table IX. Calculated and Observed Atomic Polar Tensors ($D/\text{\AA}$) for Butadiene

atom	com- ponent	d_0	d_2	d_4	d_6	av	calc
In Plane							
1	x^2	0.39	0.27	0.34	0.29	0.32 ± 0.04	0.51
1	xz	-0.60	-0.50	-0.43	-0.40	-0.48 ± 0.07	-0.67
1	zx	-0.20	-0.25	-0.25	-0.30	-0.25 ± 0.03	-0.21
1	z^2	-0.57	-0.67	-0.50	-0.56	-0.58 ± 0.05	-0.46
2	x^2	0.55	0.55	0.51	0.54	0.54 ± 0.02	0.74
2	xz	0.57	0.47	0.41	0.35	0.45 ± 0.07	0.59
2	zx	0.08	0.06	0.03	0.05	0.06 ± 0.02	-0.08
2	z^2	0.54	0.53	0.47	0.52	0.52 ± 0.02	0.59
5	x^2	-0.36	-0.30	-0.31	-0.33	-0.32 ± 0.02	-0.41
5	xz	0.39	0.36	0.38	0.39	0.38 ± 0.01	0.45
5	zx	0.12	0.10	0.09	0.12	0.11 ± 0.01	0.19
5	z^2	0.11	0.1	0.04	0.03	0.07 ± 0.04	0.06
6	x^2	-0.30	-0.23	-0.23	-0.21	-0.24 ± 0.03	-0.36
6	xz	-0.41	-0.39	-0.43	-0.43	-0.42 ± 0.02	-0.47
6	zx	-0.26	-0.26	-0.22	-0.23	-0.24 ± 0.02	-0.27
6	z^2	-0.01	0.04	0.03	0.02	0.02 ± 0.01	-0.07
7	x^2	-0.29	-0.29	-0.31	-0.29	-0.30 ± 0.02	-0.47
7	xz	0.05	0.05	0.06	0.10	0.06 ± 0.02	0.10
7	zx	0.26	0.37	0.35	0.35	0.33 ± 0.04	0.36
7	z^2	-0.06	-0.05	-0.04	-0.01	-0.04 ± 0.02	-0.12
Out of Plane (from Normal Coordinate Analysis)							
1	y^2	-1.05	-1.36	-1.13	-1.00	-1.13	-1.64
2	y^2	-0.81	-0.23	-0.64	-0.84	-0.62	-0.47
5	y^2	0.57	0.43	0.54	0.56	0.52	0.75
6	y^2	0.56	0.80	0.60	0.53	0.62	0.71
7	y^2	0.74	0.35	0.62	0.74	0.61	0.64
Out of Plane (After Fitting Frequencies and Intensities)							
1	y^2	-1.22	-1.24	-1.21		-1.22 ± 0.01	-1.64
2	y^2	-0.57	-0.52	-0.57		-0.55 ± 0.02	-0.47
5	y^2	0.52	0.51	0.53		0.52 ± 0.01	0.75
6	y^2	0.69	0.71	0.67		0.69 ± 0.02	0.71
7	y^2	0.58	0.54	0.58		0.57 ± 0.02	0.64

has not been solved in general for polyatomics in the past, and only recently with *ab initio* methods has it been possible to use intensity data from a molecule as large as butadiene. The procedure of Person and Newton was followed,²⁶ by using a set of programs written by Dempsey.²⁷ The *ab initio* atomic polar tensors (P_X , APT's) were transformed to normal coordinates

$$P_Q = P_X \times L$$

where L is the matrix of normal coordinate vectors derived by diagonalizing FG . The calculated signs and partitioning of intensity between various directions were transferred to the experimental data in order to obtain the experimental $P_Q(\partial\mu/\partial Q)$. While absolute intensities are not reproduced well by *ab initio* methods, the sign of the transition moment is usually correct in all cases with a significant moment. The experimental APT's were then obtained by using the reverse of the above transformation (Table IX). The correctness in this approach is evidenced in the good agreement between the APT's of the four isotopomers of butadiene examined. If a sign of polarization error was made it would affect the results adversely. Finally, the APT's were transformed to the dipole moment derivatives with respect to the symmetry coordinates (PS) by

$$P_S = P_X \times B^{-1}$$

where B^{-1} is the inverse of the full $3n \times 3n$ B matrix. Here, the common $3n-6 \times 3n$ symmetrized B matrix has been augmented to include the Eckart conditions which preserve the center of mass and the angular momentum during vibrations.

The consistency of the intensity data was very good except for the A_u block (y^2 , Table IX). The d_0 and d_4 compounds showed

one trend, and d_2 showed another. This was probably due to the proximity of ν_{10} and ν_{11} in the d_2 compound which causes greater mixing of the symmetry coordinates. This results in nearly degenerate eigenvalues leading to an infinite number of acceptable normal coordinate vectors, which determine intensity. In order to find a consistent set of eigenvectors (i.e., that gives consistent intensity data for all molecules) we used a steepest descent algorithm. This program used the scaled F matrix and the average P_S tensor as input and calculated the frequencies and intensities. All of the independent variables were adjusted to fit the experimental data. Due to the limited data for the d_6 molecule, it was not included. Thus 14 scale factors were used to fit 24 data points. It was necessary to choose an arbitrary weighting of the errors in frequency and in intensity in giving the overall error used to determine the steepest descent vector. The errors in frequency (in cm^{-1}) were given a weighting factor of 1, and the errors in intensity (in km/mol) were given a weighting factor of 3. A total of 20000 steps at a maximum increment of 10^{-5} was followed by 40000 at 2.5×10^{-6} , whereupon no further improvement was found. The results of this calculation are given in Tables X and XI. It is interesting to note that the F submatrix is little changed by program, except for the 10,13 element, and that the frequency fit is only slightly worse than before the changes, while the intensity data is much better. This points out a common problem in normal coordinate analyses. The form of the normal coordinate vector may not be well-defined when two vibrational modes in a given symmetry block have similar frequencies. Here, a study of the intensities of the bands provides important additional information for the relative intensities of the two bands will often be strongly dependent on the form of the normal coordinate vectors.

The dipole moment derivatives in symmetry coordinates are given in Table XII. The largest values were found with the C-H out-of-plane bending modes, S_{10} and S_{13} and with angle deformation mode, S_{24} . The out-of-plane bending modes frequently give large dipole moment derivatives with alkenes. The difference in sign between $\partial\mu/\partial S_{10}$ and $\partial\mu/\partial S_{13}$ is due to the difference in the way in which they were defined. In both cases, a hydrogen moving in the positive coordinate direction leads to an induced dipole with a positive sign. Although this suggests a C-H bond dipole in the sense C-H⁺, we have shown that it actually arises from limited orbital following with the proton moving ahead of the charge density in the overlap region.²¹ The C-H stretching modes have dipole moment derivatives which correspond to a bond dipole in the sense C⁺-H⁻, which has been found for all alkanes and alkenes. The alkynes are an exception, with a reversed sense of the dipole moment derivative for the C-H stretching modes, corresponding to the calculated reversed sign of the bond dipole.²¹

The reason for the large dipole moment derivative for S_{24} is not so clear and will be the subject of further study.

5. Spectra of Cis and Gauche Forms of Butadiene

The infrared spectra for the cis and gauche forms were calculated by using the 6-31G* basis set. Since they have a lower symmetry than *trans*-butadiene, the force constants for the latter were obtained with respect to the internal coordinates, and the dipole moment derivatives also were obtained for these coordinates.²⁸ Here, the diagonal terms of F matrix were given independent scaling factors, and the off-diagonal elements were scaled by the geometric mean of the factors for the corresponding diagonal terms.^{18a} The scaling factors for *trans*-butadiene were transferred to the calculated force constants for cis and gauche, and the vibrational frequencies were calculated giving the predicted spectra presented in Tables XIII and XIV.

The intensities were treated in a similar fashion. The theoretical $d\mu/dR$ obtained for the cis and gauche forms were scaled by the ratio of calculated to observed derivatives found for *trans*-butadiene. The predicted line intensities for the cis and gauche form also are presented in Tables XIII and XIV.

By using the data from Tables XIII and XIV, we now may construct spectra for the cis and gauche form (Figure 3). Not

(26) Person, W. B.; Newton, J. H. *J. Chem. Phys.* **1974**, *61*, 1040.

(27) Dempsey, R. Ph.D. Thesis, Yale University, 1983.

(28) These data are available as Supplementary Material.

Table X. *F* Submatrix for A_u Block Before and After Fitting, mdynes/Å

	old				new			
	10	11	12	13	10	11	12	13
10	0.3153	0.0010	-0.0101	-0.0434	0.3188	0.0010	-0.0110	-0.0638
11		0.1089	0.0200	-0.0703		0.1104	0.0194	-0.0751
12			0.2499	0.2173			0.2454	0.2136
13				0.5882				0.5950

Table XI. P_s , Frequencies, and Intensities for the A_u Block Butadiene Before and After Fitting^a

	10			11			12			13		
	initial	final	obs	initial	final	obs	initial	final	obs	initial	final	obs
P_s	1.07	1.13		0.09	0.084		0.08	0.140		-1.04	-0.98	
d_0 freq	1015.8	1014.1	1014.0	910.0	908.1	908.1	524.1	524.6	524.6	162.0	162.5	162.5
d_2 freq	913.2	908.7	908.4	852.1	850.0	850.0	480.2	487.6	480.1	138	151.8	na
d_4 freq	952.2	950.6	955.2	726.4	725.1	728.1	396.7	396.6	404	148.3	149.0	149.2
d_6 freq	773.5	758.2	766	708.1	717.8	718.6	384.6	385.4	391	127	139.7	142
d_0 int	17.8	26.87	32.4	65.3	61.56	63.0	16.0	14.59	16.2	0.12	0.14	(0.1)
d_2 int	47.7	68.68	68.9	18.8	4.93	3.6	16.7	15.38	15.2	0.05	0.07	(0.06)
d_4 int	23.4	24.42	24.5	39.8	39.67	39.8	7.9	7.79	(7.25)	0.14	0.16	(0.15)
d_6 int	1.3	0.42	(1.3)	46.3	48.59	50.1	9.1	8.84	(8.7)	0.074	0.09	(0.08)

^aThe units are as follows: P_s , D/Å; band positions, cm^{-1} ; intensities, km/mol . Intensities in parentheses are calculated values.

Table XII. Dipole Moment Derivatives in Symmetry Coordinates (D/Å) for Butadiene^a

	calc	obs	obs	obs	obs	obs
	6-31G*	But- d_0	But- d_2	But- d_4	But- d_6	av
S10	1.34	1.13	1.13	1.12		1.13 ± 0.01
S11	0.10	0.09	0.09	0.08		0.09 ± 0.01
S1i	-0.04	0.13	0.17	0.11		0.14 ± 0.02
S13	-1.05	-1.05	-0.92	-0.98		-0.98 ± 0.04
X Polarization						
S17	0.40	0.47	0.57	0.54	0.58	0.54 ± 0.04
S18	-0.64	-0.52	-0.44	-0.44	-0.48	-0.47 ± 0.03
S19	0.63	0.56	0.48	0.44	0.42	0.48 ± 0.05
S20	0.84	0.54	0.61	0.63	0.62	0.60 ± 0.03
S2u	0.08	0.11	0.10	0.13	0.10	0.11 ± 0.01
S22	0.06	0.09	0.15	0.08	0.10	0.10 ± 0.02
S23	0.09	0.07	0.13	0.12	0.14	0.12 ± 0.02
S24	0.58	0.57	0.55	0.52	0.54	0.55 ± 0.02
Z Polarization						
S17	0.66	0.67	0.73	0.64	0.73	0.69 ± 0.04
S18	0.50	0.40	0.35	0.45	0.46	0.41 ± 0.04
S19	0.62	0.50	0.44	0.49	0.50	0.48 ± 0.02
S20	-0.21	-0.11	-0.10	-0.10	-0.13	-0.11 ± 0.01
S21	-0.44	-0.44	-0.45	-0.35	-0.35	-0.40 ± 0.05
S2i	-0.28	-0.33	-0.36	-0.40	-0.37	-0.37 ± 0.02
S23	-0.05	-0.03	0.05	0.03	0.07	0.03 ± 0.02
S24	1.10	1.05	0.97	0.94	0.94	0.97 ± 0.04
Magnitude						
S17	0.77	0.82	0.92	0.81	0.92	0.87 ± 0.05
S18	0.81	0.66	0.56	0.63	0.67	0.63 ± 0.04
S19	0.88	0.75	0.65	0.66	0.66	0.68 ± 0.04
S20	0.86	0.55	0.62	0.64	0.63	0.61 ± 0.03
S21	0.45	0.46	0.45	0.36	0.35	0.40 ± 0.05
S22	0.28	0.35	0.41	0.40	0.41	0.39 ± 0.02
S23	0.10	0.07	0.15	0.14	0.16	0.13 ± 0.03
S24j	1.24	1.20	1.11	1.08	1.08	1.12 ± 0.04

^aThe values for the A_u block are those obtained after fitting frequencies and intensities simultaneously (Table X).

surprisingly the two spectra are similar overall. Minor alterations in intensity and line positions must be ignored as experimental data were obtained in a matrix, while our predictions are for the gas phase. However, one region stands out. A predicted line at 733 cm^{-1} (ν_{11}) of moderate intensity for the gauche compound is apparent in the actual experimental spectra. The closest lines for the cis compound are over 100 cm^{-1} away. The only line that accounts for this is the forbidden A_2 transition (ν_{12}) of the cis compound, which, of course, becomes allowed as the symmetry is lowered in the gauche compound. Moreover, in the d_4 and d_6 compounds this transition exists near 600 cm^{-1} (594 and 585 cm^{-1}

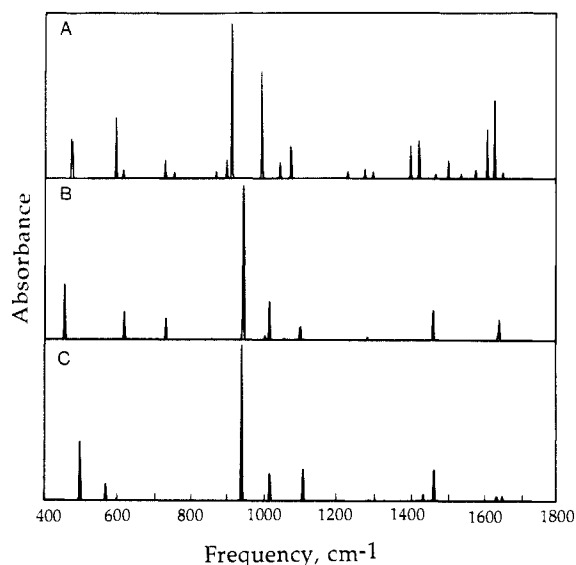


Figure 3. Spectra for butadiene rotamers. The upper plot (A) is the observed matrix isolated spectrum of the second rotamer of butadiene (ref 4). The center plot (B) is that calculated for the gauche rotamer, and the lower plot (C) is that for the cis rotamer.

predicted; 592 and 583 obs) corresponding again to the gauche species with no nearby cis transition. The fact that the weak band at 733 cm^{-1} is shifted to $\sim 600 \text{ cm}^{-1}$ in the d_4 and d_6 compounds supports the assignment of this band as ν_{11} and not some impurity.

While ab initio frequencies can be off by as much as 30 cm^{-1} , the much larger discrepancy assuming a cis form is unreasonable. We are forced to conclude that the minor rotamer of butadiene is not planar, though it need not be significantly nonplanar to fit the above data. Other data interpretations are possible. First, the crucial band may not belong to the gauche butadiene at all. However, several laboratories have assigned this band to the minor rotamer.^{3,4a,5,6} More importantly, the bands in question could be the result of a combination band. Specifically, only one combination, between ν_{13} (assuming a real vibration) and ν_{24} , would produce the appropriate frequency. This combination band does not fit our predictions nearly as well as the fundamental. Moreover, though a weak band, this band would be quite strong for a combination band.

We should note that Furukawa³ came to this same conclusion by using just an experimentally derived force field.

6. Ultraviolet Absorption Data

While the infrared data clearly indicates that the second stable conformer of butadiene is gauche, the electronic absorption data

Table XV. MELD Calculated λ_{\max} 's for Butadiene Rotamers

torsion	6-31G*				6-311 + G*			
	180.0°	38.25°	18.0°	0.0°	180.0°	40.1°	18.0°	0.0°
a. Configuration Interaction Using All Single Excitations								
E (eV)	7.22	6.96	6.54	6.43	6.14	6.22	5.65	5.49
ΔE (eV)	0.0	-0.26	-0.68	-0.79	0.0	0.08	-0.49	-0.65
$\Delta\lambda$ (nm)	0.0	10	28	33	0.0	-3	19	27
b. Configuration Interaction Using Single and Double Excitations from a Frozen Core to Lowest 18 Virtuals								
E (eV)	7.49	7.30	6.93	6.86	7.11	7.26	6.65	6.53
ΔE (eV)	0.0	-0.19	-0.56	-0.63	0.0	0.15	-0.46	-0.58
$\Delta\lambda$ (nm)	0.0	7	22	26	0.0	-5	18	23

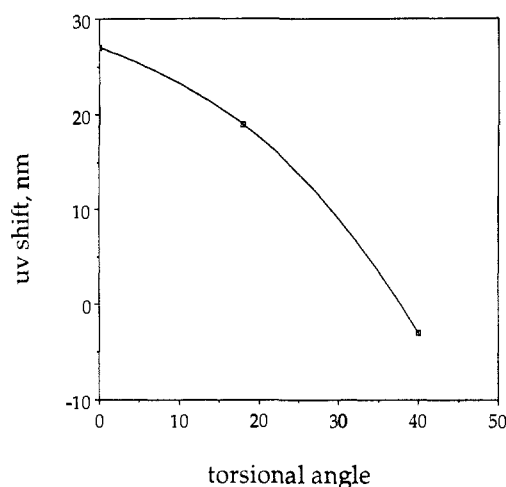
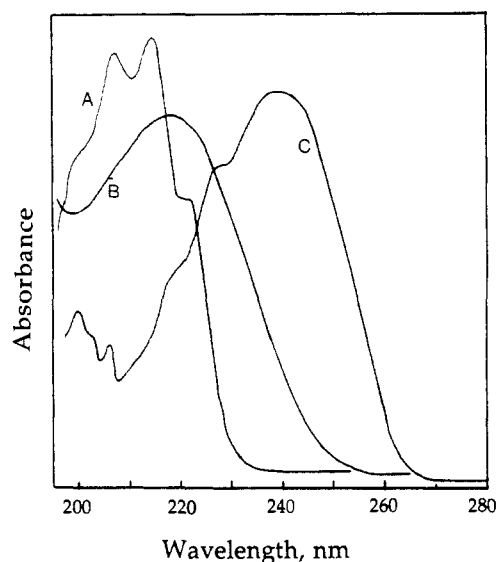


Figure 4. Calculated (CIS/6-311+G*) spectral shifts for butadiene rotamers.

λ_{\max} for butadiene at four different torsional angles. We employed two basis sets and two kinds of configuration interaction (CI) as shown in Table XV. The larger 6-311+G* basis set is better than the smaller 6-31G* basis set for two reasons. First, the diffuse functions on the larger basis set allow a better description of Rydberg character of the excited state. Cave and Davidson found a significant amount of Rydberg character in the lowest excited singlet state of butadiene. Second, the triple- ζ basis allows a better description of the virtual orbitals. The CI singles (CI-S) value is probably more reliable than the CI single and doubles (CI-SD), since the large size of the latter calculation necessitated truncation of the CI expansion beyond the 18th virtual orbital. Such truncation leads to unpredictable effects for the different rotamers studied. The important observation was that the spectral shifts obtained via the two CI methods with either basis set were comparable.

A simple interpolated three-point plot of torsion angle versus $\Delta\lambda$ for the 6-311+G* CIS values illustrates the major findings (Figure 4). The λ_{\max} of butadiene falls off slowly from a maximum value at 0° between 0° and 18° and then falls off more rapidly between 18° and 40°. With use of SSCA's value of 226 nm for the λ_{\max} of the minor isomer and 212 nm for the λ_{\max} of the major isomer, Figure 4 predicts a twist angle of 25°. With use of Saitiel's data, a twist angle of 33° is predicted. As the torsion angle changes very slowly with energy, we feel that a twist angle between 25° and 33° is close to the true torsion angle of *gauche*-butadiene.

The cisoid dienes 1,3-cycloheptadiene and 1,3-cyclooctadiene were selected as model unstrained dienes which would provide experimental backing for the above conclusions. The cycloheptadiene geometry is not known but was found by ab initio 3-21G optimizations to have nearly a 0° dihedral angle between the cis double bonds. The cyclooctadiene geometry, obtained in

Figure 5. Ultraviolet spectra (gas phase) of *trans,trans*-2,4-hexadiene (A), 1,3-cyclooctadiene (B), and 1,3-cycloheptadiene (C). The absorbance scale is arbitrary.

a similar way, had a 57° dihedral angle, a value predicted by previous MM2 calculations.³² The measured gas-phase λ_{\max} of cycloheptadiene was 242 nm (248 nm in isoctane)³³ and of cyclooctadiene 221 nm (228 nm in cyclohexane).^{21b} A similarly substituted open chain diene, *trans,trans*-2,4-hexadiene, had λ_{\max} at 214 nm (Figure 5). These data place a *gauche* form 7 nm to the red of *trans* and a *cis* form 28 nm to the red, which is consistent with the calculations shown in Figure 4. Again, they indicate that the second rotamer of butadiene should be *gauche* with a torsional angle on the order of 30°.

7. Conclusions

We have shown that ab initio predictions, vibrational data, and electronic absorption data all consistently predict a *gauche* structure for the second conformer of butadiene. The higher level of the ab initio calculations, 6-31G* to MP2/6-31G* to MP3/6-311+G**//MP2/6-31G*, the deeper the well separating the minimal *gauche* conformer from the transition-state *cis* conformer. Bands in the infrared spectra for three isotopomers of the second rotamer correspond well to predicted values for a *gauche* structure only. The λ_{\max} of electronic absorption spectra of the second rotamer, though somewhat controversial, was calculated to be consistent with a *gauche* structure with a significant twist angle and not a *cis* structure. These calculations are supported by the observed λ_{\max} of cycloheptadiene and cyclooctadiene, the former a nearly *cisoid* diene and the latter a fair model of a *gauche* structure. Though each method has minor objections, taken together all the evidence points toward a *gauche* structure with a significant dihedral angle between the two double bonds. The one experimental datum which is not compatible with a *gauche* structure is the polarization study of Michl et al.⁵ Bock and Panchenko¹⁴ have presented a detailed analysis of this experiment and have concluded that it is not able to give an unambiguous answer. In addition, since it was carried out in a matrix, it is possible that interactions with the matrix leads to a bias toward the *cis* form.

It would be very helpful to have experimental data for the second rotamer in the gas phase. It should be possible to obtain such data via supersonic jet expansion from a heated nozzle and examine the spectrum as a function of the nozzle temperature. This experiment would freeze the high-temperature rotamer population as rotationally and vibrationally cooled molecules. Although the number density of molecules in the jet would be low,

(32) (a) Cope, A. C.; Bumgardner, C. L. *J. Am. Chem. Soc.* **1956**, *78*, 2812. (b) Allinger, N. L.; Viskocil, J. R.; Burkert, U.; Yeh, Y. *Tetrahedron* **1976**, *32*, 33.

(33) Pesch, E.; Friess, S. L. *J. Am. Chem. Soc.* **1950**, *72*, 5756.

the UV cross section is sufficiently large that it should be possible to observe the change in electronic spectrum with temperature. The infrared spectrum presents more of a problem since the cross section for the bands of interest is relatively low, and since the minor rotamer will only be $\sim 10\%$ of the mixture. Nevertheless, the greatly increased sensitivity afforded by infrared diode lasers should permit the spectrum to be observed. Experiments of these types are planned.

8. Calculations

The ab initio calculations were carried out by using GAUSSIAN-86³⁴ along with standard basis sets. The calculations for the electronically excited states were carried out using the MELD package.³⁵

(34) Binkley, J. S.; Frisch, M. J.; DeFrees, D. J.; Raghavachari, K.; Whiteside, R. A.; Schlegel, H. B.; Fluder, E. M.; Pople, J. A. Department of Chemistry, Carnegie-Mellon Institute, Pittsburgh, PA.

Acknowledgment. This investigation was supported by a grant from the National Science Foundation. The calculations were carried out with a Trace computer made available via an NIH instrumentation grant. R.E.R. acknowledges an NSF predoctoral fellowship. We thank Prof. Davidson for making the MELD programs available to us, and we thank Prof Squillacote for providing the matrix isolated spectrum of butadiene.

Registry No. 1,3-Butadiene, 106-99-0; 1,3-butadiene-2,3-*d*₂, 1983-06-8; 1,3-butadiene-1,1,4,4-*d*₄, 10545-58-1; 1,3-butadiene-*d*₆, 1441-56-1.

Supplementary Material Available: Tables of internal coordinates of butadiene and F matrix from *trans*-butadiene, *cis*-butadiene, and *gauche*-butadiene (10 pages). Ordering information is given on any current masthead page.

(35) McMurdie, L. E.; Elbert, S. T.; Langhoff, S. R.; Davidson, E. R. as modified by Feller, D.; Rawlings, D. C.

Lead Sequestering Agents. 1. Synthesis, Physical Properties, and Structures of Lead Thiohydroxamato Complexes

Kamal Abu-Dari,[†] F. Ekkehardt Hahn, and Kenneth N. Raymond*

Contribution from the Department of Chemistry, University of California, Berkeley, California 94720. Received November 21, 1988

Abstract: In an approach to the synthesis of ligands specific for Pb²⁺, lead complexes with mono- and bis(thiohydroxamic acids) have been prepared and characterized on the basis of their elemental analyses and their infrared, NMR, and UV spectra. The structures of the two compounds bis(*N*-methylthiohydroxamato)lead(II) (**2**) and bis(*N*-methylthioacetohydroxamato)lead(II) (**5**) have been determined by single-crystal X-ray diffraction using automated counter methods. The structure of **2** is based on a five-coordinate geometry in which the sulfur atoms and the stereochemically active electron lone pair on Pb²⁺ occupy the equatorial positions of a trigonal bipyramid. The axial positions are occupied by the oxygen atoms and weak, outer-sphere coordination occurs from ligation by the thiohydroxamate oxygen atoms of adjacent molecules. Compound **5** exists in a similar pseudotrigonal-bipyramidal geometry in the solid state, but the equatorial positions are occupied by the lone electron pair on lead, one oxygen atom, and one sulfur atom. Additional weak coordination is formed by two oxygen atoms and one sulfur atom from neighboring molecules. Bis(*N*-methylthiohydroxamato)lead(II) (**2**) crystallizes in space group *C2/c* with *Z* = 4, *a* = 18.067 (2) Å, *b* = 12.518 (2) Å, *c* = 8.103 (1) Å and β = 101.93 (1)°. Full-matrix least-squares refinement using 1805 reflections with $F_o^2 > 3\sigma(F_o)^2$, with all non-hydrogen atoms given anisotropic temperature factors, converged to unweighted and weighted *R* factors of 1.7 and 1.9%, respectively. Bis(acetothiohydroxamato)lead(II) (**5**) crystallizes in space group *P2₁/n* with *Z* = 4, *a* = 7.958 (2) Å, *b* = 7.445 (1) Å, *c* = 19.007 (3) Å, and β = 98.74 (2)°. Full-matrix least-squares refinement using 1924 reflections with $F_o^2 > 3\sigma(F_o)^2$, with all non-hydrogen atoms given anisotropic temperature factors, converged to unweighted and unweighted *R* factors of 4.1 and 5.1%, respectively.

This paper is the first of a planned series for a research program with the goal of developing specific complexing agents for lead. To that end we will present here the background to the problems posed by lead intoxication and the chemical and biological parameters that form the boundary conditions for our ligand design.

Due to the increasing industrial uses of lead, huge amounts of lead and its compounds enter the environment each year.^{1,2} It is estimated that $\sim 3.5 \times 10^9$ kg of lead ores were mined in 1974.³ Industrial uses of lead include storage batteries, alkyllead production, cable sheathing, pigments, and lead alloys.^{2,4} Thus, even with precautions being taken, plants, animals, and humans are exposed to, and are contaminated with, lead.

Lead uptake by humans occurs through absorption of lead compounds or lead-contaminated food or drink from the gastrointestinal tract, through absorption of airborne particles through the lungs, and through absorption of lead through the skin.⁵⁻⁷ Most lead compounds are insoluble in vivo, so only small amounts

of lead are absorbed from the gastrointestinal tract. However, since it is slowly eliminated, lead accumulates in liver, kidneys, bones, and other parts of the body.⁸ The inhalation of lead compounds as lead carbonate and lead sulfate dust results in the

(1) Tsuchiya, K. In *Handbook on the Toxicity of Metals*; Friberg, L., Nordberg, G. F., Vouk, V. B., Eds.; Elsevier: North Holland, 1985; pp 452-484.

(2) Rice, H. V.; Leighty, D. A.; McLeod, G. C. *CRC Crit. Rev. Microbiol.* **1973**, *3*, 27.

(3) Moore, M. R.; Campbell, B. C.; Goldberg, A. In *The Chemical Environment*; Lenihan, J., Fletcher, W. W., Eds.; Academic Press: New York, 1977; Vol. 6, pp 64-92.

(4) Greenwood, N. N.; Earnshaw, A. *Chemistry of the Elements*; Pergamon Press: Oxford, UK, 1984.

(5) Ratcliffe, J. M. *Lead in Man and Environment*; John Wiley & Sons: New York, 1981.

(6) Luckey, T. D.; Venugopal, B.; Hutchesson, D. In *Heavy Metal Toxicity, Safety and Homology, Environmental Quality and Safety*; Coulson, F., Korte, K., Eds.; Georg Thieme Publishers: Stuttgart, 1975; Suppl. Vol. 1.

(7) Chisolm, J. J., Jr. In *Diagnosis and Treatment of Lead Poisoning*; Chisolm, J. J., Jr., et al., Eds.; Irvington: New York, 1976.

(8) Mahaffy, K. R.; Goyer, R. A. In *Diagnosis and Treatment of Lead Poisoning*; Chisolm, J. J., Jr., et al., Eds.; Irvington: New York, 1976.

* Author to whom correspondence should be addressed.

[†] On sabbatical leave from the Department of Chemistry, University of Jordan, Amman, Jordan.